Spin pumping from a ferromagnet into a hopping insulator: Role of resonant absorption of magnons

Z. Yue, D. A. Pesin, and M. E. Raikh

Phys. Rev. B **92**, 045405 — Published 6 July 2015

DOI: 10.1103/PhysRevB.92.045405

Spin pumping from a ferromagnet into a hopping insulator: the role of resonant absorption of magnons

Z. Yue, D. A. Pesin, and M. E. Raikh
Department of Physics and Astronomy, University of Utah, Salt Lake City, UT 84112, USA

Motivated by recent experiments on spin pumping from a ferromagnet into organic materials in which the charge transport is due to hopping, we study theoretically the generation and propagation of spin current in a hopping insulator. Unlike metals, the spin polarization at the boundary with ferromagnet is created as a result of magnon absorption within pairs of localized states and it spreads following the current-currying resistor network (although the charge current is absent). We consider a classic resonant mechanism of the ac absorption in insulators and adapt it to the absorption of magnons. A strong enhancement of pumping efficiency is predicted when the Zeeman splitting of the localized states in external magnetic field is equal to the frequency of ferromagnetic resonance. Under this condition the absorption of a magnon takes place within *individual* sites.

PACS numbers: 85.75.-d,72.25.Rb, 78.47.-p

I. INTRODUCTION

The phenomenon of spin pumping from a ferromagnet (F) into a normal (N) layer is one of the most prominent approaches to the generation of pure spin currents. A prime manifestation that pumping indeed takes place in realistic F-N structures is the additional broadening[1] of the ferromagnetic resonance (FMR) in F, caused by a contact with N-layer. This additional broadening was first observed experimentally in Ref. [2]. Another, more delicate, manifestation of pumping was reported shortly after. Namely, the injected spin current, entering the nonmagnetic material with spin-orbit coupling (like Pt) causes a voltage drop across the current direction. This voltage drop is due to the inverse spin-Hall effect[3] (ISHE), and has a maximum when the frequency of the microwave radiation driving the ferromagnet, ω, is equal to the FMR frequency, ω_{FMR}. Pioneering observations of pumping via ISHE in Refs. [4–6] utilized Pt as the normal layer.[7–9] They were followed by reports on similar observations of pumping into different materials[10–13], including prominent semiconductors GaAs[14], Si[15,16], Ge[17], and, most recently, graphene.[18] Experimental results on the electric field generated due to ISHE , $\boldsymbol{E}_{ISHE}$, are analyzed using the relation $\boldsymbol{E}_{ISHE} \propto \boldsymbol{J}^{(s)} \times \boldsymbol{\sigma}$, where $\boldsymbol{J}^{(s)}$ determines the spatial direction of the spin current flow and its magnitude, while $\boldsymbol{\sigma}$ is its polarization. The magnitude of the spin current is given by

$$J^{(s)} = g_{\uparrow\downarrow} C \Big[\boldsymbol{m}(t) \times \frac{d\boldsymbol{m}(t)}{dt} \Big]_z , \qquad (1)$$

where z axis is taken along the static part of the magnetization. In Eq. (1) the constant C characterizes the properties of the normal layer (like ratio of thickness to the spin-diffusion length) as well as the properties metal-ferromagnet interface, while $\boldsymbol{m}(t)$ describes the magnetization dynamics in the ferromagnet. The expression for $J^{(s)}$ has the same form as the damping term in the equation that governs $\boldsymbol{m}(t)$. It was a remarkable experimental finding[5] that ISHE voltage exhibits essentially the same behavior as a function of microwave power and the deviation of ω from ω_{FMR} as the additional FMR damping.

Microscopic physics of pumping is encoded in the mixing constant[1,19,20] $g_{\uparrow\downarrow}$ in Eq. (1). A fundamental process underlying the pumping is the inelastic electron-magnon scattering at the F-N interface. Microscopic treatment of this scattering[21,22] assumes that electrons of the normal layer impinging on the interface with ferromagnet are *plane waves*. On the other hand, in a number of recent papers[23–26] spin pumping into organic materials sandwiched between ferromagnet and Pt has been reported. Strong temperature dependence of the resistance in these materials[27] suggests that the charge transport is due to hopping of polarons[24,26], so that the description of pumping based on plane waves does not apply. This raises the question about the microscopics of spin pumping in the localized regime.

In the present paper we consider theoretically the spin pumping into a hopping insulator using the minimal model of coupling of localized states to a ferromagnet. Within this minimal model the ferromagnet is treated as a wide-gap insulator. We demonstrate that, unlike metals, the underlying process responsible for pumping is the resonant magnon absorption accompanied by transitions between localized states, see Fig. 1. A distinctive feature of pumping into an insulator is that that the pumping efficiency, commonly described by a constant, $g_{\uparrow\downarrow}$, depends strongly on the external dc magnetic field. This is because, in addition to causing the spin precession in ferromagnet, this field modifies the spin structure of the localized states between which the magnon is absorbed, see Fig. 1. The effect of external field is most pronounced when the waiting time for a hop is longer than the period of the ac field which drives the FMR. Since the resonance frequency, ω_{FMR}, depends on the orientation of the external field[28], for certain orientations[29] this frequency coincides with the Zeeman splitting of the localized states, Fig. 2. Spin pumping is most efficient for such orientations, since the absorption of magnon takes place within *individual* sites. We also show that, with no charge cur-

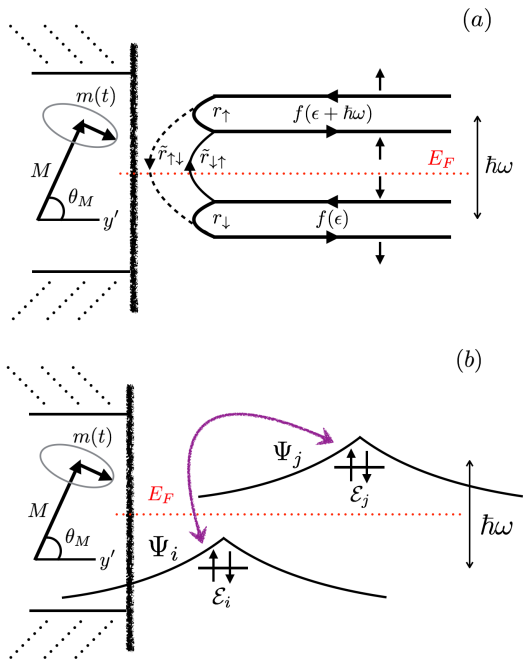

FIG. 1. (Color online) Elementary processes underlying the spin pumping into a metal (a), and into an insulator (b). In the metal, an ↑ electron, impinging on the N-F boundary, is primarily reflected elastically with amplitude $r_\uparrow$ (vertical separation of left and right arrows is a guide to an eye). Spin precession in F gives rise to inelastic reflection with amplitude $\tilde{r}_{\uparrow\downarrow}$ associated with the emission of a magnon. A ↓ electron is either reflected elastically with amplitude $r_\downarrow$, or inelastically, after absorbing of a magnon, with amplitude $\tilde{r}_{\downarrow\uparrow}$. The injected spin current is proportional to $|\tilde{r}_{\uparrow\downarrow}|^2\omega\frac{\partial f}{\partial\epsilon}$. In the insulator, only inelastic processes are at work. Emission and absorption of magnons take place within pairs of localized states.

rent, the spin polarization generated at the F-N boundary, spreads in the insulator along the same percolation network[30,31] that determines the electrical resistance.

II. ABSORPTION OF MAGNONS AT F-N BOUNDARY

A. General considerations

Figure 2 illustrates the difference between pumping into a metal, and into an insulator in an applied magnetic field, $\boldsymbol{H}$. While $\boldsymbol{H}$ is responsible for the magnetization precession in the ferromagnet, it also causes a spin splitting, Δ_z, of the spectrum in the metallic normal layer, Fig. 2a. This splitting, however, does not affect the absorption of magnons. The reason is that the absorption at a boundary does not require momentum conservation, i.e. the matrix element is constant, and thus there is no dependence of the spin current, $I^{(s)}$, on the dc field in the normal layer.

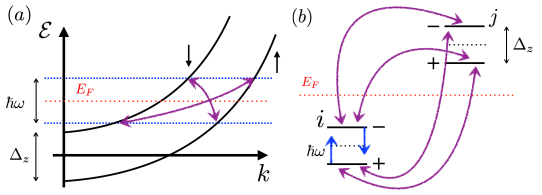

FIG. 2. (Color online) Illustration of pumping in metal (a) and in insulator (b) in the presence of a Zeeman splitting, Δ_z. In metal, the absorption (emission) of a magnon, $\hbar\omega$, near the F-N boundary does not conserve momentum, and thus is insensitive to the ratio $\Delta_z/\hbar\omega$. By contrast, in and insulator, and near the condition $\hbar\omega = \Delta_z$, the absorption (emission) of a magnon is *resonant*.

The situation is different for an insulator, where the magnon absorption takes place between the discrete levels, Fig. 2(b). In this case, and for a general orientation of $\boldsymbol{H}$, the Zeeman levels are the linear combinations of ↑ and ↓ spin states. As a result, transitions from *each* of the initial states on site i to *both* final states on site j are allowed. This fact distinguishes absorption of magnons from the conventional absorption of an ac *electric* field[32–34], and, as we will see below, gives rise to $\boldsymbol{H}$-dependence of the spin current. Another origin of $\boldsymbol{H}$-dependence is the possibility of *intrasite* absorption of magnons at the boundary. We will see that the intrasite transitions dominate the absorption near the resonant condition $\hbar\omega = \Delta_z$. Away from this condition, the intersite transitions dominate.

B. The model

Consider a pair of localized states, i and j, Fig. 2(b). Assume for simplicity that the ferromagnet is an insulator, i.e. it is a barrier for electrons in N. Precession, $\boldsymbol{m}(t)$, of magnetization in ferromagnet can be modeled as a time-dependent correction $\propto \boldsymbol{m}(t)\hat{\sigma}$ to the barrier potential. The pumping takes place since the wave function, Ψ_i, can penetrate under the barrier. As a result, the Hamiltonian of site i has a correction

$$\delta\hat{H}_i = J\Big[\hat{\sigma}_x m_x \sin\omega t + \hat{\sigma}_y m_y \cos\omega t\Big], \qquad (2)$$

where J accounts for tunneling. Projections $m_x(t)$ and $m_y(t)$ are proportional to the magnitude of the microwave field and depend in a resonant way on the proximity of ω to ω_{FMR}. Analytical expressions for these projections can be found e.g. in Ref. [9].

The Hamiltonian $\delta\hat{H}_i$ of Eq. (2) causes transitions of electrons between the sites i and j. Absorption of energy in course of these transitions is quite similar to the absorption of the ac *electric* field by pairs of the localized states. However, the transitions caused by $\delta\hat{H}_i$ are accompanied by spin flips, both from ↑ to ↓, and from ↓ to ↑. With regard to absorption of energy, one should add

up the contributions of the both types of transitions, i.e.

$$I^{(e)} = I_{\downarrow\to\uparrow} + I_{\uparrow\to\downarrow} \tag{3}$$

However, the spin current results from the fact that these contributions are not equal to each other, so that

$$I^{(s)} = I_{\downarrow\to\uparrow} - I_{\uparrow\to\downarrow}. \tag{4}$$

Thus, for calculation of the spin current into hopping insulator, one can use the standard "resonant" phononless absorption theory[32] and substitute the corresponding rates into Eq. (4).

C. Resonant absorption at $\boldsymbol{H} = 0$

We first neglect the Zeeman splitting in the normal layer. In this case resonant transitions happen within pairs of localized states, Fig. 1b. The correction $\delta\hat{H}_i$ causes such transitions between the sites i and j because the corresponding wave functions $|i\rangle$ and $|j\rangle$ have a finite overlap integral, t_{ij}.[33] Due to this overlap, the eigenfunctions of the pair get modified as

$$\begin{aligned} |\mathbf{i}\rangle &= \sqrt{\frac{\Gamma+\delta\varepsilon}{2\Gamma}}|i\rangle + \sqrt{\frac{\Gamma-\delta\varepsilon}{2\Gamma}}|j\rangle, \\ |\mathbf{j}\rangle &= -\sqrt{\frac{\Gamma-\delta\varepsilon}{2\Gamma}}|i\rangle + \sqrt{\frac{\Gamma+\delta\varepsilon}{2\Gamma}}|j\rangle, \end{aligned} \tag{5}$$

for $\delta\varepsilon = \varepsilon_j - \varepsilon_i > 0$. The corresponding energies are

$$\tilde{\varepsilon}_{i,j} = \frac{\varepsilon_i+\varepsilon_j}{2} \mp \frac{\Gamma}{2}, \quad \Gamma = \left[\delta\varepsilon^2 + 4t_{ij}^2\right]^{1/2}. \tag{6}$$

Since both modified eigenfunctions contain $|i\rangle$, the matrix element of $\delta\hat{H}_i$ between them is finite, and the Golden-rule expression for the spin-flip part of the $i\to j$ transition rate for $\varepsilon_j > \varepsilon_i$ reads

$$I^{(s)}_{i\to j} = -m_x m_y J^2 \mathrm{F}(\tilde{\varepsilon}_i, \tilde{\varepsilon}_j, \omega), \tag{7}$$

where the function F is defined as

$$\begin{aligned} \mathrm{F}(\tilde{\varepsilon}_i, \tilde{\varepsilon}_j, \omega) &= \frac{2t_{ij}^2}{(\tilde{\varepsilon}_j - \tilde{\varepsilon}_i)^2} \frac{\frac{1}{\tau}[f(\tilde{\varepsilon}_i) - f(\tilde{\varepsilon}_j)]}{(\tilde{\varepsilon}_j - \tilde{\varepsilon}_i - \hbar\omega)^2 + \left(\frac{\hbar}{\tau}\right)^2} \\ &= \frac{2t_{ij}^2}{\Gamma^2} \frac{\frac{1}{\tau}[f(\tilde{\varepsilon}_i) - f(\tilde{\varepsilon}_j)]}{(\Gamma - \hbar\omega)^2 + \left(\frac{\hbar}{\tau}\right)^2}. \end{aligned} \tag{8}$$

Here we have introduced the phonon broadening of the levels, τ^{-1}.

It is easy to see that the transition rate to states with $\varepsilon_j < \varepsilon_i$ is given by Eq. (7) with function F from Eq. (8), but with $f(\tilde{\varepsilon}_i) \leftrightarrow f(\tilde{\varepsilon}_j)$, and thus the rate has the same sign as Eq. (7). Physically, this can be seen from the following argument: Consider the simple case of $m_x = m_y$. The Hamiltonian of Eq. (2) implies that for a given site at the interface, spins $\uparrow$ are transferred to states of higher energy (and there is a backflow of spins $\uparrow$ converted from $\downarrow$ from those states), while spins $\downarrow$ are pushed to states with lower energy (and there is a backflow of spins $\downarrow$ converted from $\uparrow$). Since the occupation of the state at the interface is larger than of those at higher energy, there is a negative $\downarrow\to\uparrow$ conversion rate because of transitions up the energy. This is exactly what Eq. (7) suggests. Further, since the occupation of the state at the interface is lower than of those at lower energy, there is a positive $\uparrow\to\downarrow$ conversion rate, or, again, negative $\downarrow\to\uparrow$ one. Hence a simple permutation $f(\tilde{\varepsilon}_i) \leftrightarrow f(\tilde{\varepsilon}_j)$ suffices to describe transitions to states with $\varepsilon_j < \varepsilon_i$.

The product $m_x m_y$ in Eq. (7) is specific for spin pumping, see Eq. (1). The expression for the net absorption rate contains $\frac{1}{2}(m_x^2 + m_y^2)$ instead. Another difference from the conventional resonance absorption[31,32] is the structure of the matrix element in Eq. (7). This, however, modifies the result of averaging over the sites, j, only by a numerical factor. A crucial observation in the averaging procedure[32] is that the relevant sites, j, are located within a narrow spherical layer with a radius r_ω which is found from the condition $2|t_{ij}(r_\omega)| = \hbar\omega$. Assuming the exponential decay of the overlap integral with distance, $|t_{ij}(r)| = t_0 \exp(-r_{ij}/a)$, we have

$$r_\omega = a \ln \frac{2t_0}{\hbar\omega}. \tag{9}$$

The result of averaging and summing over sites far away from the boundary reads

$$I^{(s)}(\omega) = 2\pi^2 m_x m_y J^2 \left(g\omega a r_\omega^2\right) \frac{\partial f}{\partial \varepsilon}, \tag{10}$$

where g is the density of states. The transition rate of Eq. (10) should be interpreted as the spin current generated per a localized state coupled to the ferromagnet.

D. Resonant absorption at finite $\boldsymbol{H}$

To generalize Eq. (7) to a finite magnetic field in the normal layer, one must take into account the modification of the spin eigenstates, as well as the Zeeman splitting in energies of the latter. The spin structure of the spin-split levels depends on the orientation of $\boldsymbol{H}$ as follows

$$|\chi_{\mathbf{H}+}\rangle = \cos\Big(\frac{\theta_H - \theta_M}{2}\Big)|\chi_{\mathbf{M}+}\rangle + i\sin\Big(\frac{\theta_H - \theta_M}{2}\Big)|\chi_{\mathbf{M}-}\rangle, \tag{11}$$

$$|\chi_{\mathbf{H}-}\rangle = \cos\Big(\frac{\theta_H - \theta_M}{2}\Big)|\chi_{\mathbf{M}-}\rangle + i\sin\Big(\frac{\theta_H - \theta_M}{2}\Big)|\chi_{\mathbf{M}+}\rangle. \tag{12}$$

Here the quantization axes for $|\chi_{\mathbf{M}\pm}\rangle$ and $|\chi_{\mathbf{H}\pm}\rangle$ spinors are chosen along the static part of the magnetization, and the external magnetic field, respectively, see Fig. 3(a). The states $|\chi_{\mathbf{M}\pm}\rangle$ at sites i and j are split by Δ_z.

All four transitions between states with $|\chi_{\mathbf{M}\pm}\rangle$ spin wave functions, Fig. 2(b), are allowed for a general orientation of the magnetic field. For spin-conserving transitions ($+\to+$ and $-\to-$), the frequency dependence of $I^{(s)}$ remains ωr_ω^2, i.e. the same as in Eq. (10). Orientation of $\boldsymbol{H}$ enters into the prefactor: The product $m_x m_y$ should be replaced with $\frac{1}{4}\sin^2(\theta_H-\theta_M)m_x^2$ for both transitions.

While the spin-conserving transitions do affect the spin current density distribution in the sample, they are non-resonant, and it is the spin-flipping ones ($+\leftrightarrow-$) that are responsible for the spin current generation at the interface. In other words, no spin current is possible in a stationary state without the latter processes. Therefore, in what follows we concentrate on the frequency and magnetic field dependence of the corresponding rates.

As far as $+\to-$ and $-\to+$ transitions are concerned, only the $+\to-$ with absorption of a magnon, and $-\to+$ with emission of a magnon become important in the vicinity of the resonance $\hbar\omega=\Delta_z$. The other two transitions are non-resonant, and therefore disregarded here. For the $+\leftrightarrow-$ transitions, the prefactor ω in the spin current remains intact, since it comes from the difference in the populations of levels involved. However, despite the upper and lower Zeeman levels being separated in energy, the overlap of the spatial wave functions is determined by ε_i, ε_j in *zero* magnetic field. Thus, the $+\to-$ transitions take place between pairs with $(\varepsilon_j-\varepsilon_i)\sim|\hbar\omega-\Delta_z|$. These pairs have the "shoulder"

$$r_{\hbar\omega-\Delta_z}=a\ln\frac{2t_0}{|\hbar\omega-\Delta_z|}. \tag{13}$$

Logarithmic divergence of Eq. (13), which is cut off at $|\hbar\omega-\Delta_z|\sim\hbar/\tau$, ensures the resonant character of spin-flipping transitions that we took into account.

In addition to the replacement of r_ω by $r_{\omega-\Delta_z}$ in the spin current, the prefactor $m_x m_y$ should be modified as $m_x m_y\to \mathrm{G}(m_x,m_y)$, where the function G is defined as

$$\mathrm{G}(m_x,m_y)=\tfrac{1}{4}(m_x+m_y\cos(\theta_H-\theta_M))^2, \tag{14}$$

so that the absorption, and thus the FMR damping, do not have the usual form $\propto m_x m_y$.

The most spectacular manifestation of the resonance $\hbar\omega=\Delta_z$ is that the *intrasite* transitions become possible, as illustrated in Fig. 2(b). For these transitions the overlap of the spatial parts of the on-site wave functions is equal to 1, and the magnetic-field dependence of absorption is a pure Lorentzian. Orientation-dependent prefactor, which is the matrix element of $\delta\hat{\mathcal{H}}_i$ between the spinors $|\chi_{\mathbf{H}+}\rangle$ and $|\chi_{\mathbf{H}-}\rangle$ is the same as in Eq. (14). Summarizing, we present the expression for spin current close to the resonance $\hbar\omega=\Delta_z$ in the form

$$I^{(s)}(\omega)=2\mathrm{G}(m_x,m_y)J^2\omega\frac{\partial f}{\partial\varepsilon}\times\left[\frac{\frac{\hbar}{\tau}}{(\Delta_z-\hbar\omega)^2+\left(\frac{\hbar}{\tau}\right)^2}+\pi^2 g a^3\ln^2\frac{2t_0}{|\hbar\omega-\Delta_z|}\right], \tag{15}$$

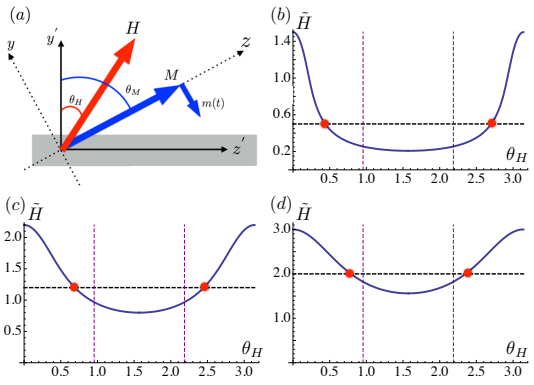

FIG. 3. (Color online) (a) The geometry of FMR; For a fixed dimensionless frequency, $\tilde{\omega}=\omega_{FMR}/4\pi M_s$, the dimensionless magnitude, $\tilde{H}=H/4\pi M_s$, and orientation, θ_H, of dc magnetic field are related via Eq. (17). This dependencies are shown for the values of $\tilde{\omega}/\gamma$: (b) 0.5, (c) 1.2, and (d) 2. Red dots indicate the values of H, for which the condition $\gamma H=\omega_{FMR}$ is satisfied.

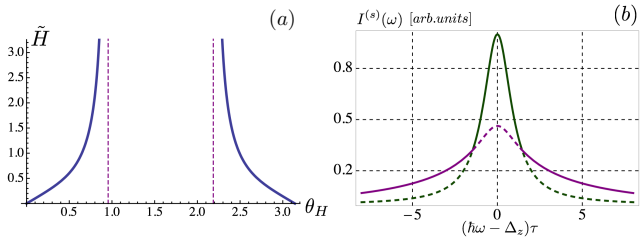

FIG. 4. (Color online) (a) the resonant condition $\gamma H=\omega_{FMR}$ is satisfied along the solid lines on the $\left(\frac{H}{4\pi M_s}\right)-\theta_H$ plane. The cutoff values of θ_H are $\cos^{-1}\left(\frac{1}{\sqrt{3}}\right)\approx 55^\circ$ and $\pi-\cos^{-1}\left(\frac{1}{\sqrt{3}}\right)$. (b) the behavior of the spin current calculated from Eq. (15) for $ga^3\hbar/\tau=4\cdot10^{-3}$ and $t_0\tau/\hbar=15$.

where the first term comes from intrasite and the second term from intersite transitions. Directly at the resonance, the first term dominates. This is ensured by the condition $ga^3\hbar/\tau\ll1$. Since the combination $1/ga^3$ is the minimal energy spacing between two sites in the insulator located within $\sim a$ from each other, the above condition implies that this spacing is much bigger than the phonon broadening of individual levels, which is the definition of the Anderson insulator. As the deviation from the resonance increases, the behavior of $I^{(s)}(\omega)$ is dominated by the second term. Neglecting the logarithm, the crossover takes place at $|\Delta_z-\hbar\omega|\tau/\hbar\gtrsim\left(\tau/\hbar ga^3\right)^{1/2}\gg1$. The behavior of spin current near the resonance is shown in Fig. 4(b), where the logarithm was cut off at $|\hbar\omega-\Delta_z|=t_0/15$.

III. RESONANT ORIENTATIONS OF EXTERNAL FIELD

Equation (15) is our main result. To make connection to the experimental papers Refs. [23–26], below we calculate the magnitude and orientation of the dc field where the anomalous behavior of ISHE voltage takes place. Such behavior takes place when two conditions are met: The Zeeman splitting of the localized states is equal to $\hbar\omega$, and $\omega = \omega_{FMR}$.

We specify the orientation of $\boldsymbol{H}$ and magnetization, $\boldsymbol{M}$, using the notations common in the literature, see e.g. Refs. [9, 15, and 24], and Fig. 3. We will also introduce dimensionless variables $\tilde{H}$, $\tilde{M}$ and $\tilde{\omega}$, which stand for H, M and ω_{FMR} in the units of $4\pi M_s$, where M_s is the saturation magnetization. Then the angle θ_M, corresponding the equilibrium orientation of $\boldsymbol{M}$, is found from the condition that $\boldsymbol{M}$ is parallel to the effective magnetic field, with the demagnetizing term taken into account[9]

$$2\tilde{H}\sin(\theta_H - \theta_M) + \sin 2\theta_M = 0, \tag{16}$$

while the expression for the resonant frequency, $\tilde{\omega}$, reads[28]

$$\left(\frac{\tilde{\omega}}{\gamma}\right)^2 = \left[\tilde{H}\cos(\theta_H - \theta_M) - \cos 2\theta_M\right] \times \left[\tilde{H}\cos(\theta_H - \theta_M) - \cos^2\theta_M\right]. \tag{17}$$

From these two equations we exclude θ_M and plot the dimensionless field $\tilde{H}$ versus θ_H, for a *given* FMR frequency $\tilde{\omega}$. Examples of these curves are shown in Fig. 3. Resonant orientation is obtained by crossing a curve $\tilde{H}(\theta_H)$ by the line $\tilde{\omega} = \gamma\tilde{H}$. Two intersections determine the orientations for which ω_{FMR} is equal to the Zeeman splitting of the localized states. Upon changing ω_{FMR}, we get two lines of resonances, Fig. 4(a). They occupy two domains: $0 < \theta_H < \cos^{-1}\frac{1}{\sqrt{3}}$ and $(\pi - \cos^{-1}\frac{1}{\sqrt{3}}) < \theta_H < \pi$. At the boundaries of the domains $\tilde{H}$ goes to infinity. Then it follows from Eqs. (16) and (17) that at these boundaries $\sin(\theta_M - \theta_H) = 0$, and θ_H satisfies the equation $\cos(2\theta_H) + \cos^2\theta_H = 0$, yielding $\theta_H = \cos^{-1}\left(\frac{1}{\sqrt{3}}\right) \approx 55°$.

In Refs. [23 and 24] on pumping into organics the microwave frequency driving the resonance was 9.45 Ghz, while the values of $4\pi M_s$ were very different, namely, $4\pi M_s = 0.175$ T in Ref. [23] and $4\pi M_s = 0.805$ T in Ref. [24]. Then from Fig. 4(a) we find that the resonant angle θ_H should be close to 45° for Ref. [23] and 23° for Ref. [24].

IV. SPIN-RESISTOR NETWORK

After the spin polarization is generated at the boundary, it should spread into the bulk of the insulator to avoid the backflow.[35] In a metal, where $\boldsymbol{P}$ is a continuous function of coordinates, this spreading is by spin diffusion accompanied by the Larmor precession. In a hopping insulator $\boldsymbol{P}$ takes discrete values, $\boldsymbol{P}_i$, which are the polarizations on the sites, i. The Larmor precession is accounted for by the on-site Zeeman splitting, Δ_z, of the levels, see Fig. 2. The frequencies of electron hops between two sites, i and j, depend strongly on their energies, ε_i, ε_j, and their spatial separation, r_{ij}. Then the issue of spreading of the spin polarization reduces to the question: what is the spin current $\boldsymbol{I}^{(s)}_{i\to j}$ between the sites with polarizations $\boldsymbol{P}_i$ and $\boldsymbol{P}_j$, provided that, on average, there is no charge current between these sites?

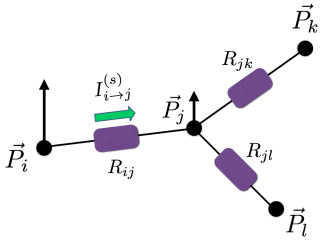

FIG. 5. (Color online) "Spin-resistor" network. Polarizations $\boldsymbol{P}_i$ and $\boldsymbol{P}_j$ on the sites i, j determine the spin current between these sites. The coefficients, R_{ij}, are proportional to the electric hopping resistances.

If bias were applied between the two sites, then the average charge current, proportional to this bias, could be found by ascribing an effective resistance, R_{ij}, to the pair of sites[30,31]. It is easy to see that the same R_{ij} determines the proportionality coefficient between $\boldsymbol{I}^{(s)}_{i\to j}$ and $\boldsymbol{P}_i - \boldsymbol{P}_j$, namely

$$\boldsymbol{I}^{(s)}_{i\to j} = 2\frac{\boldsymbol{P}_i - \boldsymbol{P}_j}{R_{ij}\frac{\partial f}{\partial \varepsilon}}. \tag{18}$$

In Eq. (18) we have assumed that the difference $(\varepsilon_i - \varepsilon_j)$ is much smaller than the temperature, so that $\frac{\partial f}{\partial \varepsilon}$ is the same for both sites. Equation (18) follows from the fact that the on-site chemical potentials of the local majority and minority electrons are shifted by $\mp|\boldsymbol{P}_i|/\frac{\partial f}{\partial \varepsilon}$, respectively. The spinors that correspond to these local spin eigenstates are defined by the directions of $\boldsymbol{P}_i$, $\boldsymbol{P}_j$. Importantly, the fact that the chemical potential splitting is symmetric around the chemical potential of the unpolarized system ensures the absence of the charge current, i.e. the net current flow $i \to j$ is compensated by the net current flow $j \to i$. With different spin polarizations of the sites, the compensation of the charge flows leads to the imbalance of the spin flows, and thus to Eq. (18). Note that Eq. (18) remains valid in external magnetic field, which enters only via the magnitudes of polarizations. Overall, Eq. (18) suggests that polarization built up at the F-N boundary spreads along the current-carrying resistor network, as illustrated in Fig. 5.

V. CONCLUDING REMARKS

(i) Our result Eq. (15) applies when the phonon-induces broadening of the levels is smaller than ω. In the opposite case, $\omega\tau \ll 1$, the mechanism of absorption is the Pollak-Geballe relaxation mechanism, Ref. [36]; no sharp dependence of pumping near the resonance is expected in this regime. Unlike pumping into metals, the pumping rate Eq. (15) is not simply proportional to $\boldsymbol{m} \times \frac{d\boldsymbol{m}}{dt}$. The prefactor in Eq. (14) depends on the relative orientation of $\boldsymbol{m}$ and the external magnetic field, $\boldsymbol{H}$.

(ii) Suppose that we are at resonance $\hbar\omega = \Delta_z$. The microwave field acts both by driving the FMR but also directly, by causing transitions between the Zeeman levels. If the amplitude of the field in frequency units (Rabi frequency) exceeds the inverse spin relaxation time, these transitions will be saturated in the bulk. Then the pumping becomes inefficient.

(iii) In conventional theory of hopping transport the applied voltage drops not on all the resistors constituting the network, but on the highest, critical, resistors representing the "hardest" hops.[31] The spin relaxation rate will be dominated by hyperfine or spin-orbit environment[37,38] of this hop.

(iv) We did not consider effects of electron-electron interaction, and did not describe in detail how finite resistance of the spin-current network, Section IV, affects the measured value of the spin current. In brief, Coulomb correlations enhance the absorption of magnons by increasing the number of singly occupied pairs[33], while the measured spin current is given by Eq. (15) only in the limit of vanishingly small bulk resistance. These considerations are, however, completely standard, and do not change the qualitative picture of spin current generation by resonant magnon absorption in hopping insulators, developed in this paper.

Acknowledgements. We are grateful to C. Boehme and Z. V. Vardeny for piquing our interest in the subject. The work was supported by NSF grants MRSEC DMR-1121252 (ZY and MER), and DMR-1409089 (DAP).

[1] Y. Tserkovnyak, A. Brataas, and G. E. W. Bauer, Phys. Rev. Lett. **88**, 117601 (2002).
[2] S. Mizukami, Y. Ando, and T. Miyazaki, Phys. Rev. B **66**, 104413 (2002).
[3] M. I. Dyakonov and A. V. Khaetskii, in *Spin Physics in Semiconductors*, ed. by M. I. Dyakonov, Chapter 8 (Springer, Berlin, 2008).
[4] E. Saitoh, M. Ueda, H. Miyajima, and G. Tatara, Appl. Phys. Lett. **88**, 182509 (2006).
[5] H. Y. Inoue, K. Harii, K. Ando, K. Sasage, and E. Saitoh, J. Appl. Phys. **102**, 083915 (2007).
[6] K. Ando, S. Takahashi, K. Harii, K. Sasage, J. Ieda, S. Maekawa, and E. Saitoh, Phys. Rev. Lett. **101**, 036601 (2008).
[7] K. Ando, T. Yoshino, and E. Saitoh, Appl. Phys. Lett. **94**, 152509 (2009).
[8] J.-C. Rojas-Sánchez, N. Reyren, P. Laczkowski, W. Savero, J.-P. Attané, C. Deranlot, M. Jamet, J.-M. George, L. Vila, and H. Jaffrès, Phys. Rev. Lett. **112**, 106602 (2014).
[9] K. Ando, S. Takahashi, J. Ieda, Y. Kajiwara, H. Nakayama, T. Yoshino, K. Harii, Y. Fujikawa, M. Matsuo, S. Maekawa, and E. Saitoh, J. Appl. Phys. **109**, 103913 (2011).
[10] O. Mosendz, J. E. Pearson, F. Y. Fradin, G. E. W. Bauer, S. D. Bader, and A. Hoffmann, Phys. Rev. Lett. **104**, 046601 (2010).
[11] B. Heinrich, C. Burrowes, E. Montoya, B. Kardasz, E. Girt, Y.-Y. Song, Y. Sun, and M. Wu, Phys. Rev. Lett. **107**, 066604 (2011).
[12] J.-C. Lee, L.-W. Huang, D.-S. Hung, T.-H. Chiang, J. C. A. Huang, J.-Z. Liang, and S.-F. Lee, Appl. Phys. Lett. **104**, 052401 (2014).
[13] J. E. Gómez, B. Z. Tedlla, N. R. Álvarez, G. Alejandro, E. Goovaerts, and A. Butera, Phys. Rev. B **90**, 184401 (2014).
[14] A. Yamamoto, Y. Ando, T. Shinjo, T. Uemura, and M. Shiraishi, Phys. Rev. B **91**, 024417 (2015).
[15] K. Ando and E. Saitoh, Nat. Commun. **3**, 629 (2012).
[16] E. Shikoh, K. Ando, K. Kubo, E. Saitoh, T. Shinjo, and M. Shiraishi, Phys. Rev. Lett. **110**, 127201 (2013).
[17] S. Dushenko, M. Koike, Y. Ando, T. Shinjo, M. Myronov, and M. Shiraishi, arXiv:1501.06691.
[18] S. Singh, A. Ahmadi, C. T. Cherian, E. R. Mucciolo, E. del Barco, and B. Özyilmaz, Appl. Phys. Lett. **106**, 032411 (2015).
[19] A. Brataas, Yu. V. Nazarov, and G. E. W. Bauer, Phys. Rev. Lett. **84**, 2481 (2000).
[20] Y. Tserkovnyak, A. Brataas, G. E. W. Bauer, and B. I. Halperin Rev. Mod. Phys. **77**, 1375 (2005).
[21] M. D. Styles and A. Zangwill, Phys. Rev. B **66**, 014407 (2002).
[22] S. A. Bender and Y. Tserkovnyak, arXiv:1409.7128.
[23] K. Ando, S. Watanabe, S. Mooser, E. Saitoh, and H. Sirringhaus, Nat. Mater. **12**, 622 (2013).
[24] S. Watanabe, K. Ando, K. Kang, S. Mooser, Y. Vaynzof, H. Kurebayashi, E. Saitoh, and H. Sirringhaus, Nat. Phys. **10**, 308 (2014).
[25] Z. Qiu, M. Uruichi, D. Hou, K. Uchida, H. M. Yamamoto, E. Saitoh, arXiv:1502.05244.
[26] M. Kimata, D. Nozaki, Y. Niimi, H. Tajima, and Y. Otani, arXiv:1411.2740.
[27] For example, the bulk resistance, $\rho(T)$, in Ref. [26] increased by two orders of magnitude between the room temperature and 20 K following the Mott's law $\ln \rho \propto T^{-1/4}$. The localization length inferred by the authors from the transport measurements is quite small: $a \approx 11$ nm.
[28] C. Kittel, Phys. Rev. **73**, 155 (1948).
[29] R. H. Silsbee, A. Janossy, and P. Monod, Phys. Rev. B **19**, 4382 (1979). The authors demonstrate theoretically and experimentally that paramagnetic resonance in copper foil is greatly enhanced when the Zeeman frequency coincides with the frequency of FMR in ferromagnet coupled to the foil.
[30] V. Ambegaokar, B. I. Halperin, and J. S. Langer, Phys.

Rev. B **4**, 2612 (1971).
[31] B. I. Shklovskii and A. L. Efros, *"Electronic Properties of Doped Semiconductors"* (Springer-Verlag, Berlin, 1984).
[32] N. F. Mott, Philos. Mag. **22**, 7 (1970).
[33] A. L. Efros and B. I. Shklovskii, in *Electron-Electron Interactions in Disordered Systems*, edited by A. L. Efros and M. Pollak North-Holland, Amsterdam, 1985.
[34] B. I. Shklovskii and A. L. Efros, Zh. Eksp. Teor. Fiz. **81**, 406 (1981) [Sov. Phys. JETP **54**, 218 (1981)].
[35] A. Brataas, Y. Tserkovnyak, G. E. W. Bauer, and B. I. Halperin, Phys. Rev. B **66**, 060404(R) (2002).
[36] M. Pollak and T. H. Geballe, Phys. Rev. **122**, 1742 (1961).
[37] N. J. Harmon and M. E. Flatté Phys. Rev. Lett. **110**, 176602 (2013).
[38] R. C. Roundy and M. E. Raikh Phys. Rev. B **88**, 205206 (2013).